

## Article

# Roman Wall Paintings: Characterisation of Plaster Coats Made of Clay Mud

Roberto Bugini <sup>1</sup>, Cristina Corti <sup>2,\*</sup> , Luisa Folli <sup>1</sup> and Laura Rampazzi <sup>1,2</sup> 

<sup>1</sup> Institute for Heritage Science (ISPC), National Research Council (CNR), Via Roberto Cozzi 53, 20125 Milan, Italy; bugini@icvbc.cnr.it (R.B.); lufolli@gmail.com (L.F.)

<sup>2</sup> Department of Human Sciences and Innovation for the Territory, Università degli Studi dell'Insubria, Via Sant'Abbondio 12, 22100 Como, Italy; laura.rampazzi@uninsubria.it

\* Correspondence: cristina.corti@uninsubria.it

**Abstract:** This paper reports on the mineralogical characterisation of samples of wall paintings from various Roman sites in Lombardy (Italy), revealing recurrent types of stratigraphy. One of the stratigraphic samples analysed was found to be a particular kind of plaster: a three-coat work featuring two coats made of clay mud, found in the site of *Santa Maria alla Porta* (area of the Imperial Palace of Milan—first century CE). The fragments were analysed using optical microscopy on thin sections, X-ray diffraction, scanning electron microscopy with an energy-dispersive spectrometer and infrared spectroscopy, also in non-invasive external reflection mode (7500–375 cm<sup>-1</sup>). The most interesting feature found was the finish coat made of clay mud (illite, chlorite, kaolinite and fine quartz) with a few coarse clasts and linear cavities. This clay coat was the first example ever detected in Roman Lombardy and was used in combination with a thin painted coat made of clay mud with coarse clasts together with a blue pigment (Egyptian blue) and a render coat made of lime associated with lithic clasts (sand). Our findings brought to light a particular construction technique, since in the historical sources clay is only recommended for daubing on reeds and as a render coat.



**Citation:** Bugini, R.; Corti, C.; Folli, L.; Rampazzi, L. Roman Wall Paintings: Characterisation of Plaster Coats Made of Clay Mud. *Heritage* **2021**, *4*, 889–905. <https://doi.org/10.3390/heritage4020048>

Academic Editor: Carlos Alves

Received: 29 April 2021

Accepted: 19 May 2021

Published: 20 May 2021

**Publisher's Note:** MDPI stays neutral with regard to jurisdictional claims in published maps and institutional affiliations.



**Copyright:** © 2021 by the authors. Licensee MDPI, Basel, Switzerland. This article is an open access article distributed under the terms and conditions of the Creative Commons Attribution (CC BY) license (<https://creativecommons.org/licenses/by/4.0/>).

**Keywords:** clay mud; plaster coat; Roman plaster; wall paintings; Egyptian blue; FTIR; SEM-EDX; XRD; reflectance infrared spectroscopy; thin sections

## 1. Introduction

Roman painted plasters made up of overlying coats are reported by Vitruvius and by Pliny in a sequence containing: a render coat, made of lime as binder together with coarse sand as aggregate (sand from river deposits—*harenatum*); a finish coat, made of lime as the binder with fine marble powder as the aggregate (crushed calcite crystals—*marmoratum*); and a painted coat as the top layer [1–3]. A significant feature of these recipes is the change in aggregate composition between the render coat and the finish coat.

Archaeometric studies on Roman archaeological sites of the present-day region of Lombardy (corresponding to the eastern part of *X Regio Venetia* and to the western part of *XI Regio Transpadana*) have reported on various plasters that match to some extent the guidelines of Vitruvius and Pliny [4]. The difference in the composition between the render coats (silicate sand) and the finishing coats (calcite powder) was very often in accordance with the guidelines; however, the number of coats was significantly reduced (two or, rarely, three coats) [5]. Other kinds of aggregate were also employed (i.e., a *marmoratum* made of crystals of quartz instead of crystals of calcite).

We carried out a systematic campaign of mineralogical analyses on numerous samples of wall paintings from various Roman sites in Lombardy (northern Italy). The results, along with the description and comparison of the mortars, led to the identification of recurrent types of stratigraphy. An excavation recently made in the area of the former *Palatium* (Imperial Palace) in *Mediolanum* (Milan, Italy) (Figure 1) unearthed erratic fragments coming from the painted plaster showing two anomalous coats made of clay mud. Despite

the extensive literature, even in recent years, describing analyses conducted on Roman wall paintings [6–13], to the best of our knowledge nothing similar has ever been characterised before. Using microscopic and chemical investigations, we focused on these particular fragments in order to characterise a Roman building technique never described so far in the literature.

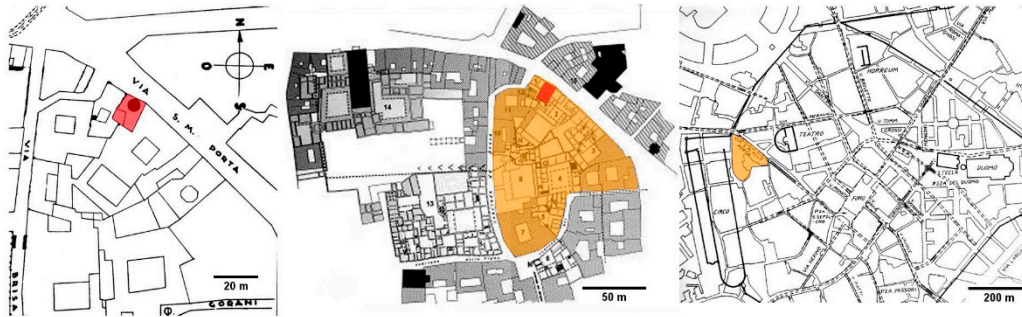


**Figure 1.** The location of the site of *Santa Maria alla Porta* (Milan, Italy). The investigated site and the *Palatium* are marked in red and orange colour, respectively. The map is shown at different levels of magnification (see scale bars) to help to situate the site in the Roman city structure.

In this paper, we report our analysis of the wall paintings from various Roman sites and describe our analytical campaign conducted on the particular samples from Milan, comparing it with our previous analyses [4,5,14]. The analyses were carried out with optical microscopy on thin sections, X-ray diffraction on powders and on fragments specifically treated for clay analysis, scanning electron microscopy equipped with an energy-dispersive spectrometer and infrared spectroscopy. Infrared measurements were also made in external reflection mode (FTIR-ER), typically used for non-invasive characterisation of painted surfaces, but rarely for wall paintings [9,11,12,15–20].

#### The archaeological site

A district of the Roman town of *Mediolanum* (Milan, Italy) was occupied by a vast complex of buildings, known as the *Palatium*, which was built in the first century CE and encircled by the urban walls on the northern side and bordered by the *circus* on the western side (Figure 1). Very little is left of the *Palatium*: the most significant remains are located in via Brisa and consist of a circular colonnaded peristyle surrounded by some rooms of different shapes. The excavations carried out in 2015 in the northern part of the Imperial Palace area (via Santa Maria alla Porta 3, near via Brisa), unearthed a rubbish heap containing fragments of painted plasters mixed with other materials. These remains were from the first century CE, and their destruction was caused by the work on the Imperial building. The site was unearthed, cleaned out, studied and then covered because it was not possible to musealise the archaeological remains. The samples here analysed were labelled by the archaeologists as erratic fragments of the wall paintings present at the site.

Our main interest was on some fragments of wall paintings featuring a three-coat work together with a blue pigment (Figure 2).

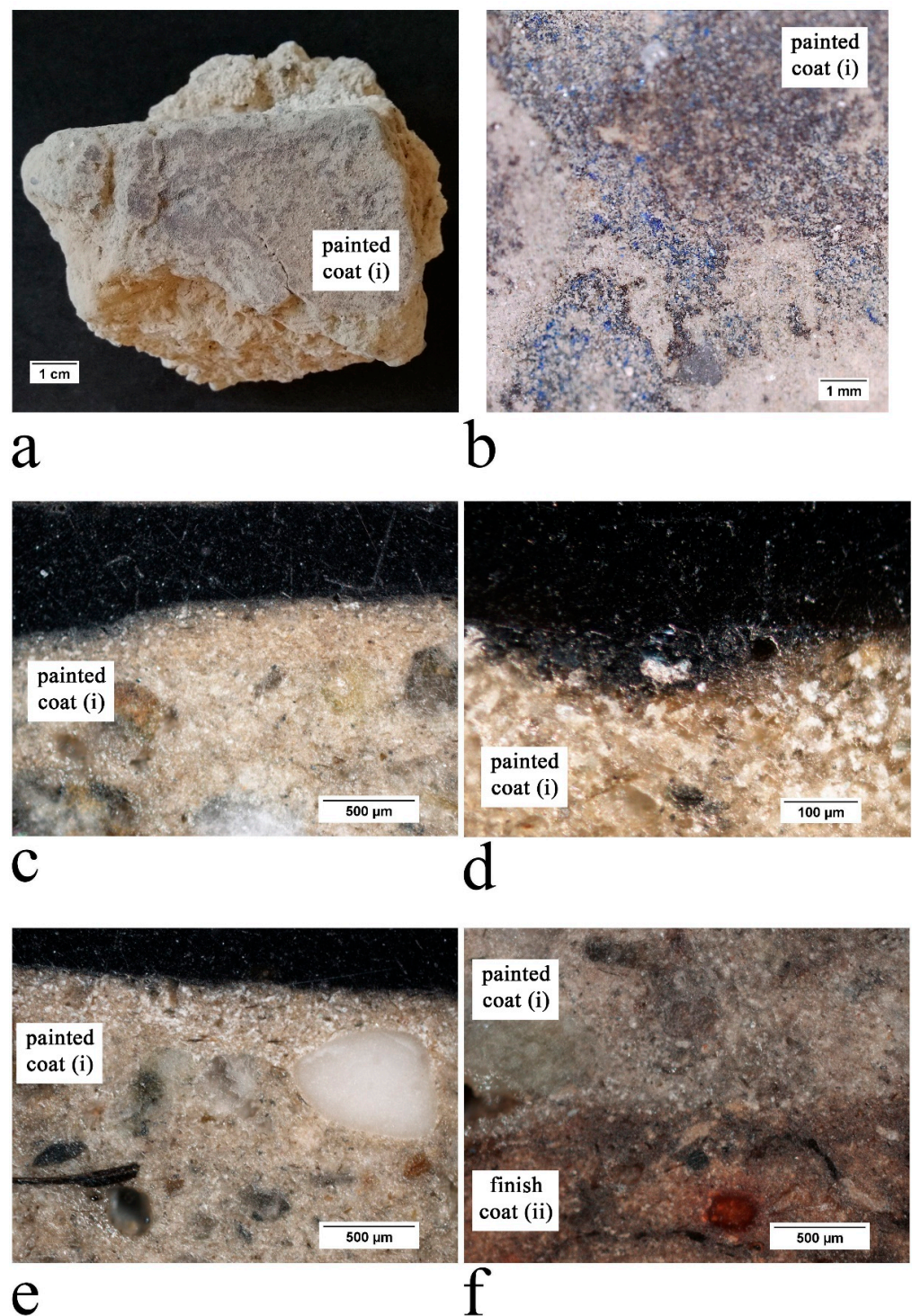


**Figure 2.** (a) Painted surface of the sample and (b) digital microscope image of the painted surface: a mixture of blue and black particles can be seen; (c–e) optical microscope image of layer (i) (polished cross section); (f) optical microscope image of layer (ii) and layer (i) (polished cross section).

## 2. Materials and Methods

Samples of each plaster coat were analysed as thin sections using optical microscopy (polarised light), as powders and fragments with X-ray diffraction and infrared spectroscopy, as polished cross sections with scanning electron microscopy and optical microscopy, ‘as is’ with external reflection infrared spectroscopy and digital portable microscopy.

### Optical microscopy

The painted layer was observed with digital portable microscope MAOZUA USB001 and images were acquired using the software MicroCapture Plus (Mustech Electronics Co., Ltd., Shenzhen, China).

Thin sections were prepared according to the standard method. Nikon Eclipse E400Pol equipped with Nikon Pol objectives was used for the observation.

A fragment of sample was embedded in an epoxy resin, cross-cut with a diamond saw and then mechanically polished. The polished cross section was then observed with an optical microscope, Nikon Eclipse LV150, equipped with a Nikon DS-FI1 digital image acquisition system. Images were acquired and elaborated using the NIS-elements F software.

#### **Scanning Electron Microscopy and Energy Dispersive X-ray spectroscopy**

A sample prepared as a polished cross section was observed with a FEI/Philips XL30 ESEM (low vacuum mode (1 torr), 20 kV, BSE detector) [21,22]. The elemental analyses were carried out using an X-ray energy dispersive spectrometer, EDAX AMETEK Element, coupled to SEM.

#### **X-ray diffraction**

The samples were analysed as fine ground powders using a Rigaku MiniFlex 300 diffractometer (Rigaku Americas Corporation, The Woodlands, TX, USA) (30 kV, 10 mA, Cu-K $\alpha$  radiation ( $\lambda = 1.5418 \text{ \AA}$ ), 5–55° Theta/2-Theta, step scan 0.02°, scan speed 3°/min). PDXL2 software supporting ICDD (International Centre for Diffraction Data) PDF2 databases were used to identify the phases.

Some fragments were processed for clay mineral analysis too [23,24] as follows: dilution in water (30 mL); coarse grains removal by wet sieving (71 micrometres sieve); first analysis of dried specimens; exposition (two hours) to ethylene glycol (about 60 °C); cooling; exposition (two hours) in a muffle furnace (about 550 °C); cooling and second analysis; treatment with hydrochloric acid; third analysis. The instrument was a PANalytical X'Pert PRO MPD: generator settings 40 mA and 40 kV; radiation Cu-Ka  $\lambda = 1.5406 \text{ \AA}$ ; scan range 3–35° 2 $\theta$ ; step size 0.017 2 $\theta$ ; scan step time 10.3376 s; continuous scan type; software PANalytical X'Pert HighScore.

#### **Infrared spectroscopy**

FTIR-ATR spectra were acquired by means of a Thermo Scientific Nicolet iS10 instrument (Thermo Fisher Scientific, Waltham, MA, USA), in the range between 4000 and 600 cm<sup>-1</sup>, 4 cm<sup>-1</sup> resolution, 32 scans. The background was periodically registered.

FTIR measurements in external reflection mode (FTIR-ER) were carried out on the surface of the fragments with an Alpha Bruker FTIR portable spectrophotometer, equipped with a DTGS detector. The optimal distance was achieved by checking the focus via the on-board camera. Subsequently, a finer tuning was achieved via software, looking for the maximum signal directly in the interferogram. The average working distance from the surface was about 1–1.5 cm. Spectra were collected between 7500 and 375 cm<sup>-1</sup>, with 4 cm<sup>-1</sup> resolution and 200 scans. The background was periodically acquired using a flat gold mirror.

Both FTIR-ATR and FTIR-ER spectra were interpreted by comparison with a home-made reference database and with the literature [25,26].

### **3. Results**

Table 1 reports the results of our systematic campaign of mineralogical analysis of wall paintings from Roman sites in Lombardy.

With regards to the site at *Santa Maria alla Porta*, the features of the samples are described, starting with the painted coat, i.e., the external layer.

**Table 1.** Description and main mineralogical features of the analysed plasters coming from Roman archaeological sites in Milan and Brescia.

Site	Number of Samples with the Same Stratigraphy	Chronology (Century *)	Plaster Thickness (mm)	Render Coat: Aggregate Composition	Finish Coat			Pigment
					Binder Composition	Aggregate Composition	Crystal Size (mm)	
<b>Milano</b>								
Università Cattolica	6	1st	12–30	quartz, silicates, limestone	Mg lime	quartz, limestone, brick	0.04–3.0	not examined
Università Cattolica	17	3rd	18–35	quartz, silicates, brick	Mg lime	calcite, quartz, silicates	0.04–2.7 0.1–3.0	not examined
piazza Fontana	6	mid 1st	20–35	quartz, silicates	Mg lime	quartz, silicates	1.0–3.0	cinnabar, carbon black
piazza Fontana	2	early 1st	25	quartz, silicates	Mg lime	quartz	0.1–3.0	carbon black
piazza Meda	2	mid 1st	25–30	quartz, silicates, brick	Mg lime	quartz	0.4	red ochre
piazza Meda	1	early 4th	28	quartz, silicates, brick	Mg lime	quartz	0.4	green earth
via Correnti	9	1st	15–25	quartz, silicates, limestone	Mg lime	quartz, silicates, limestone	0.1–1.2	green earth
via Correnti	25	2nd	15–20	quartz, silicates, limestone	Mg lime	quartz, limestone, calcite	0.05–2.5 0.04–2.0	green earth, yellow ochre
via Broletto	9	3rd	15–22	quartz, silicates	Mg lime	quartz, silicates, calcite	0.05–0.4	cinnabar, red ochre, green earth
corso Magenta (Monastero Maggiore)	10	3rd	25–55	quartz, silicates, brick	Mg lime	quartz, calcite	0.1–2.0	red ochre
corso Magenta (palazzo Litta)	6	3rd	40–45	quartz, silicates	Mg lime	quartz	1.0–3.0	Egyptian blue, green earth, red ochre, carbon black
via S. Maria Porta	3	3rd	15–60	quartz, silicates	Mg lime	calcite	0.2–1.5	cinnabar, yellow ochre, Egyptian blue
<b>Brescia</b>								
Under the Sanctuary	6	2nd BCE	2–5	limestone, gneiss	Mg lime	quartz, limestone	0.4	red earth, carbon black, chalk

Table 1. Cont.

Site	Number of Samples with the Same Stratigraphy	Chronology (Century *)	Plaster Thickness (mm)	Render Coat: Aggregate Composition	Finish Coat			Pigment
					Binder Composition	Aggregate Composition	Crystal Size (mm)	
Sanctuary	34	early 1st BCE	5–10	quartz, limestone, dolomite	Ca lime	dolomite	0.3–3.0	yellow ochre, red earth, Egyptian blue + green earth, cinnabar, carbon black
Sanctuary	18	early 1st BCE	20–25	limestone, quartz, brick	Ca lime	clay + quartz	0.1–0.3	Egyptian blue, red ochre
Sanctuary	1	early 1st	30	limestone, flint	Ca lime	dolomite, limestone	0.3–3.0	not examined
via Trieste	6	mid 1st	2–3	quartz, limestone	Mg lime	calcite	1.5	red earth, green earth, yellow ochre
palazzo Martinengo	7	early 1st	4–5	limestone	Mg lime	dolomite	0.3–3.5	red earth, Egyptian blue + green earth
palazzo Martinengo	14	late 1st	4–13	quartz, limestone	Mg lime	dolomite	0.3–4.0	Egyptian blue + green earth, red earth
Liceo Arnaldo	19	mid 1st–early 2nd	4–8	dolomite	Mg lime	dolomite	0.5–1.5	red earth, green earth, yellow ochre
Santa Giulia	42	late 2nd–early 3rd	3–11	dolomite	Mg lime	dolomite	0.3–2.5	green earth, yellow ochre, Egyptian blue
<b>Brescia Province</b>								
<b>Cividate Camuno</b>								
via Palazzo	9	1st	10–20	quartz, silicates	Mg lime	calcite, limestone	0.1–3.5	red ochre, yellow ochre, Egyptian blue

Table 1. Cont.

Site	Number of Samples with the Same Stratigraphy	Chronology (Century *)	Plaster Thickness (mm)	Render Coat: Aggregate Composition	Finish Coat			Pigment
					Binder Composition	Aggregate Composition	Crystal Size (mm)	
Theatre	5	late 1st	5	quartz, limestone, brick	Mg lime	calcite	0.1–1.0	red earth
<i>domus</i>	7	mid 1st	10–20	quartz, limestone	Mg lime	calcite	0.3–4.0	not examined
Amphitheatre	10	early 1st	5–15	quartz, limestone	Mg lime	calcite	0.3–4.0	red ochre, green earth
Sanctuary of Minerva-Breno	18	1st	10–20	quartz, limestone	Mg lime	calcite	0.1–3.5	red ochre, yellow ochre, Egyptian blue
<b>Sirmione-Villa Grotte di Catullo</b>	19	2nd	15–50	limestone	Ca lime	calcite, limestone	0.2–4.0 0.2–0.6	Egyptian blue, cinnabar, red and yellow ochre, minium (lead), green earth, carbon back
<b><i>Bedriacum</i></b>								
<i>domus</i>	20	1st–2nd	15–20	quartz, limestone	Ca lime	brick, calcite, limestone	0.4–5.0 0.1–0.8	yellow ochre, red earth, green earth
Rubble pit	8	1st–5th	10–20	quartz, limestone	Mg lime	quartz, limestone, brick	0.5–5.0	red ochre, red earth, chalk

**Legend:** Ca lime: calcitic lime; Mg lime: magnesian lime; \* site chronology is intended to be CE unless otherwise indicated.

#### (i) Painted coat

Based on the observation of thin sections, the paint layer contains a pigment made of Egyptian blue ( $\text{CaCuSi}_4\text{O}_{10}$ , calcium copper silicate—synthetic analogous of cuprorivaite). This layer lies on a coat (thickness 4 mm) containing clay mud with a homogeneous texture and small irregular cavities (size 0.2–0.4 till 1.0 mm) (Figure 3). Figure 4 shows the XRD analyses of the samples processed for clay mineral analysis. Kaolinite is destroyed upon heating, while as for illite and chlorite no change at all in the peak position and shapes is observed, except for the disappearance of the chlorite signal at 4.68 Å [23,24]. Thus, the clay is made up of these minerals. Angular quartz (size 0.05 mm) is present as well. There are also many coarse clasts of quartz, gneiss, limestone and marble (sub-angular corners, low sorting, size from 0.2 to 1.5 mm).

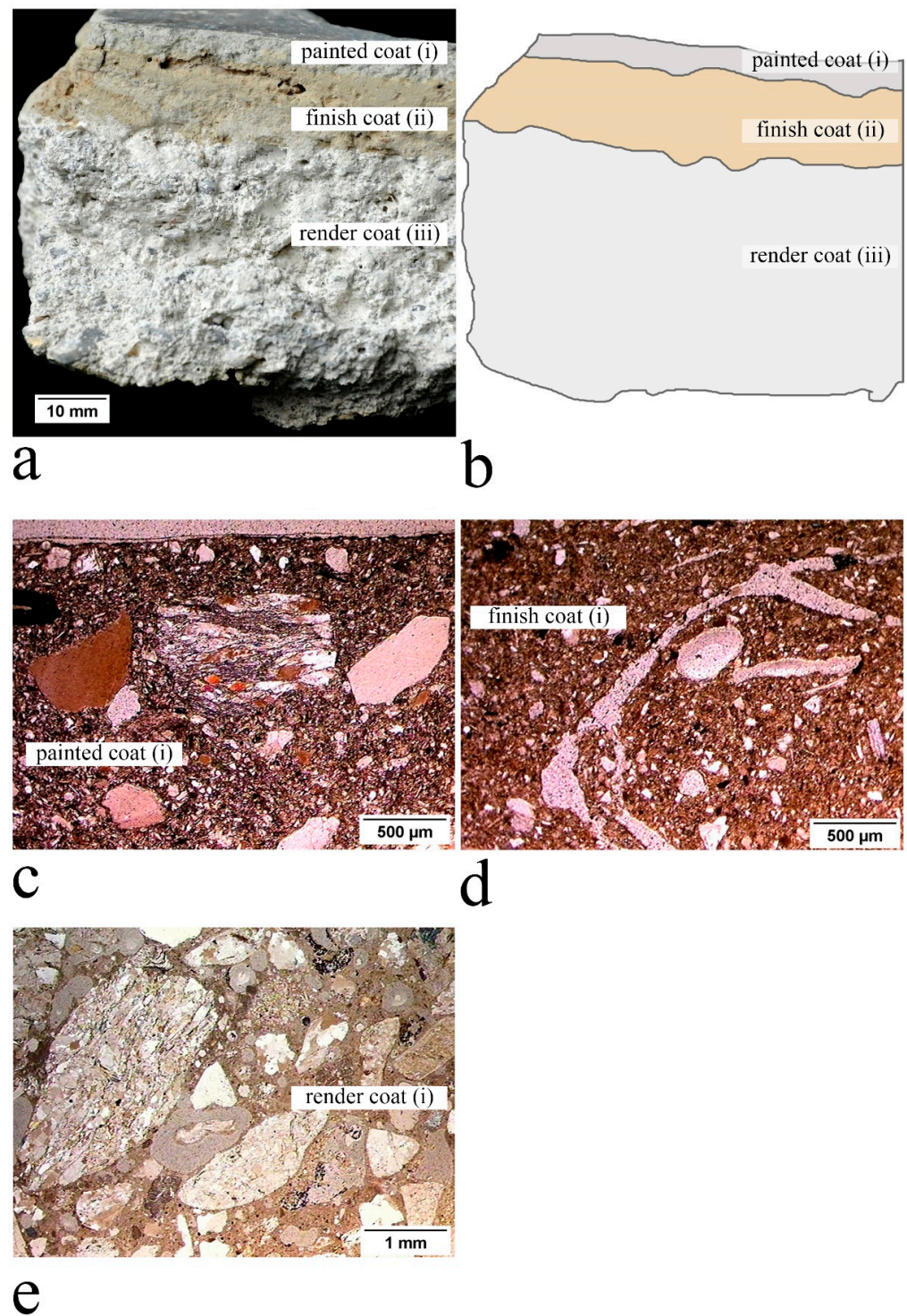


**Figure 3.** (a,b) A sample from the site of *Santa Maria alla Porta*, showing the sequence of the plaster coats: (i) painted (top, thin); (ii) finish (middle); (iii) render (bottom, thick). (c) Thin cross sections of the painted coat (i) with clay mud and coarse clasts. (d) Finish coat (ii) with clay mud and linear cavities. (e) Render coat (iii) with lime and lithic clasts (optical microscopy plane-polarised light).

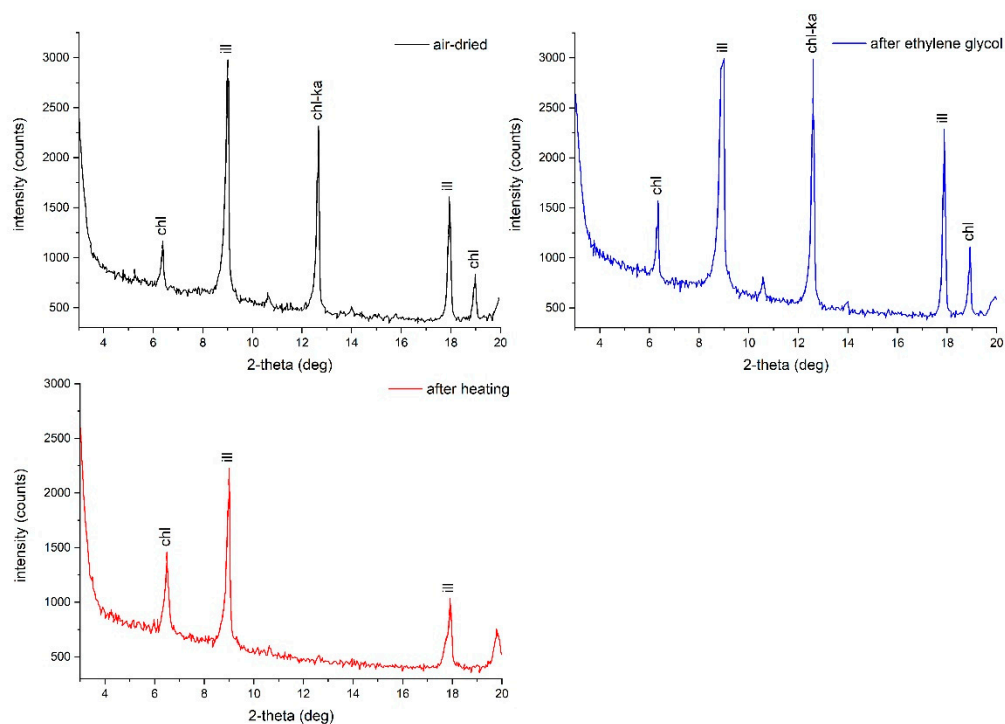


**Figure 4.** XRD analysis of a sample from the painted coat (i) processed for clay mineral analysis. Diffractograms of the air-dried sample (**top, left**), after exposition to ethylene glycol (**top, right**) and after heating (**bottom, left**). Legend: chl: chlorite; ill: illite; ka: kaolinite.

The FTIR spectrum in ATR mode of the same layer (Figure 5) shows an intense peak at  $997\text{ cm}^{-1}$  and a smaller one at  $1161\text{ cm}^{-1}$ , which resemble the antisymmetric Si-O-Si stretching modes of Egyptian blue [27]. The signals at  $760$  and  $671\text{ cm}^{-1}$  are likely due to the symmetric stretching of the same group, and thus are confirmatory. The absorbance peaks at  $1418$ ,  $874$  and  $713\text{ cm}^{-1}$  (C-O asymmetric stretching, out-of-plane bending and in-plane bending vibrations, respectively) show the presence of calcium carbonate from the substrate [28,29]. The doublet at  $795$  and  $778\text{ cm}^{-1}$  and the signal at  $694\text{ cm}^{-1}$  (Si-O symmetrical stretching and bending vibrations, respectively) resemble quartz, present as an impurity of the pigment or in the aggregate fraction of the mortar [26].

The FTIR-ER analysis (Figure 5) confirmed the presence of calcium carbonate, as can be seen from the bands at  $713\text{ cm}^{-1}$  (C-O symmetric in-plane bending),  $875\text{ cm}^{-1}$  (C-O asymmetric out-of-plane bending),  $1453\text{ cm}^{-1}$  (C-O asymmetric stretching),  $1796\text{ cm}^{-1}$  (combination band),  $2519\text{ cm}^{-1}$  and its shoulder at  $2585\text{ cm}^{-1}$  (combination bands) and  $4261\text{ cm}^{-1}$  (overtone) (Figure 5) [11,30]. There are quartz peaks at  $469\text{ cm}^{-1}$  (Si-O asymmetric bending),  $521\text{ cm}^{-1}$  (Si-O asymmetric bending),  $695$  and  $793\text{ cm}^{-1}$  (Si-O symmetric stretching),  $810\text{ cm}^{-1}$  (Si-O bending),  $1158\text{ cm}^{-1}$  (Si-O asymmetric stretching),  $1873$  and  $1990\text{ cm}^{-1}$  [30,31]. Kaolinite, found in the clay-based support, is particularly evident from peaks at  $3697$  and  $3623\text{ cm}^{-1}$  (O-H group vibrations) and  $911\text{ cm}^{-1}$  (Si-O stretching) [12,15]. The presence of gypsum at the surface was not detected either from ATR or XRD, but can be inferred from peaks at  $2136$  and  $2236\text{ cm}^{-1}$  (overtone and combination bands) [15,30]. The peak at  $1624\text{ cm}^{-1}$  is either gypsum or an unidentifiable organic substance (other peaks can be seen at  $2987$ ,  $2930$  and  $2877\text{ cm}^{-1}$ ).

The identification of Egyptian blue pigment signals was complicated both by the small amounts of pigment on the surface and by the presence of other silicates in the substrate. The peaks at  $1159\text{ cm}^{-1}$  (Si-O asymmetric stretching),  $1047\text{ cm}^{-1}$  (Si-O asymmetric stretching),  $998\text{ cm}^{-1}$  (Si-O asymmetric stretching),  $751$  and  $673\text{ cm}^{-1}$ , fit our Egyptian blue reference and other references reported in the literature [15]. The peak at  $1283\text{ cm}^{-1}$  may be related either to an unidentified organic treatment or possibly to Egyptian blue [32] or gypsum [12].

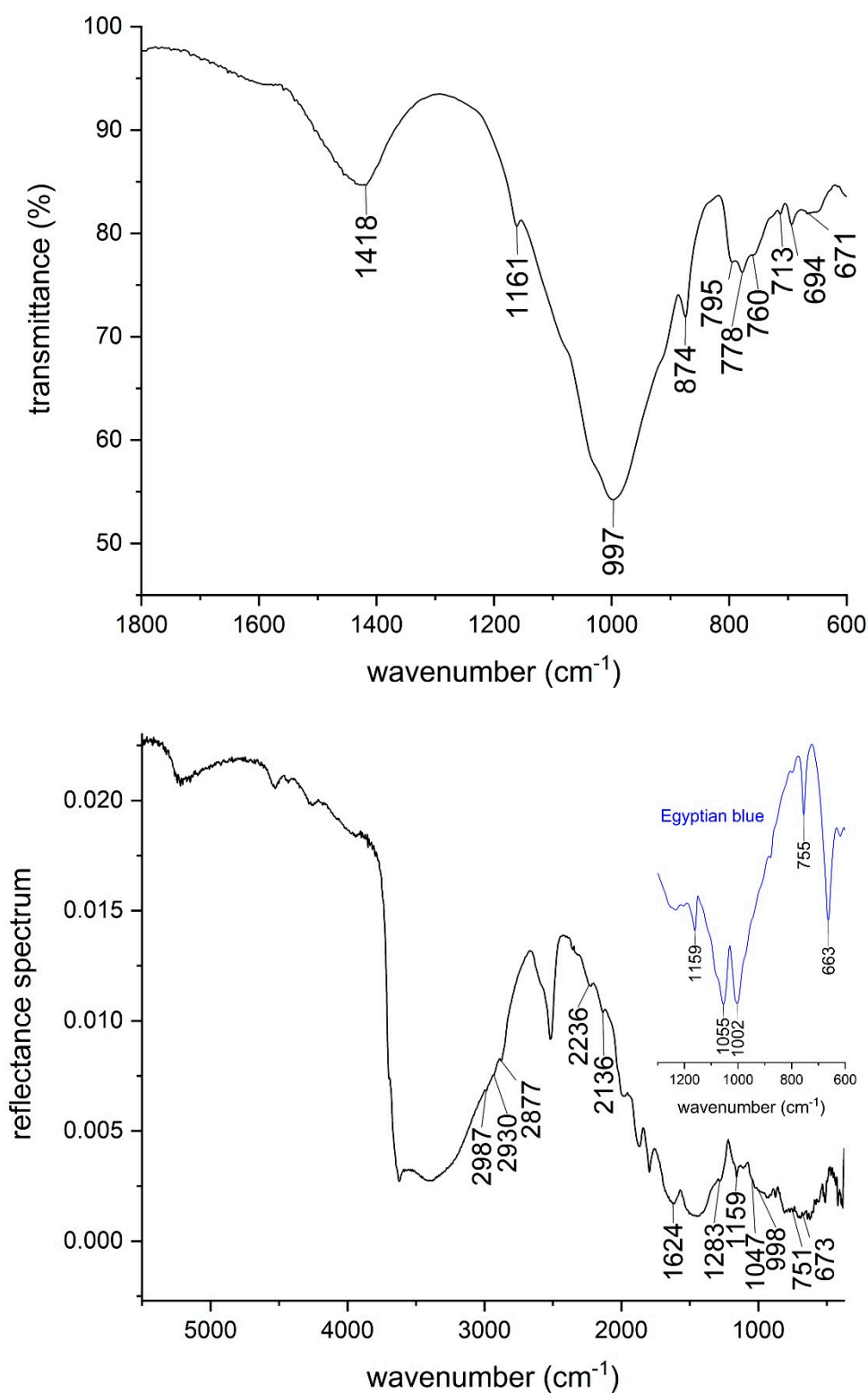


**Figure 5.** ATR spectrum (**top**) of the painted layer, showing the presence of Egyptian blue (1161, 997, 760 and 671  $\text{cm}^{-1}$ ), calcite (1418, 874 and 713  $\text{cm}^{-1}$ ) and quartz (795, 778 and 694  $\text{cm}^{-1}$ ); FTIR-ER spectrum (**bottom**) of the painted coat, with the most interesting peaks. Peaks of Egyptian blue (1159, 1047, 998, 751, 673  $\text{cm}^{-1}$ —see also an excerpt of FTIR-ER spectrum of Kremer 10060 Egyptian blue standard pigment), gypsum (2136, 2236  $\text{cm}^{-1}$ ) and organic substance (2987, 2939, 2877  $\text{cm}^{-1}$ ) were shown.

XRD analysis of powders detected quartz, calcite, illite, albite, kaolinite and chlorite. There are also some weak peaks that may be related to cuprorivaite (Egyptian blue) and magnetite (black earth) (Figure 6).

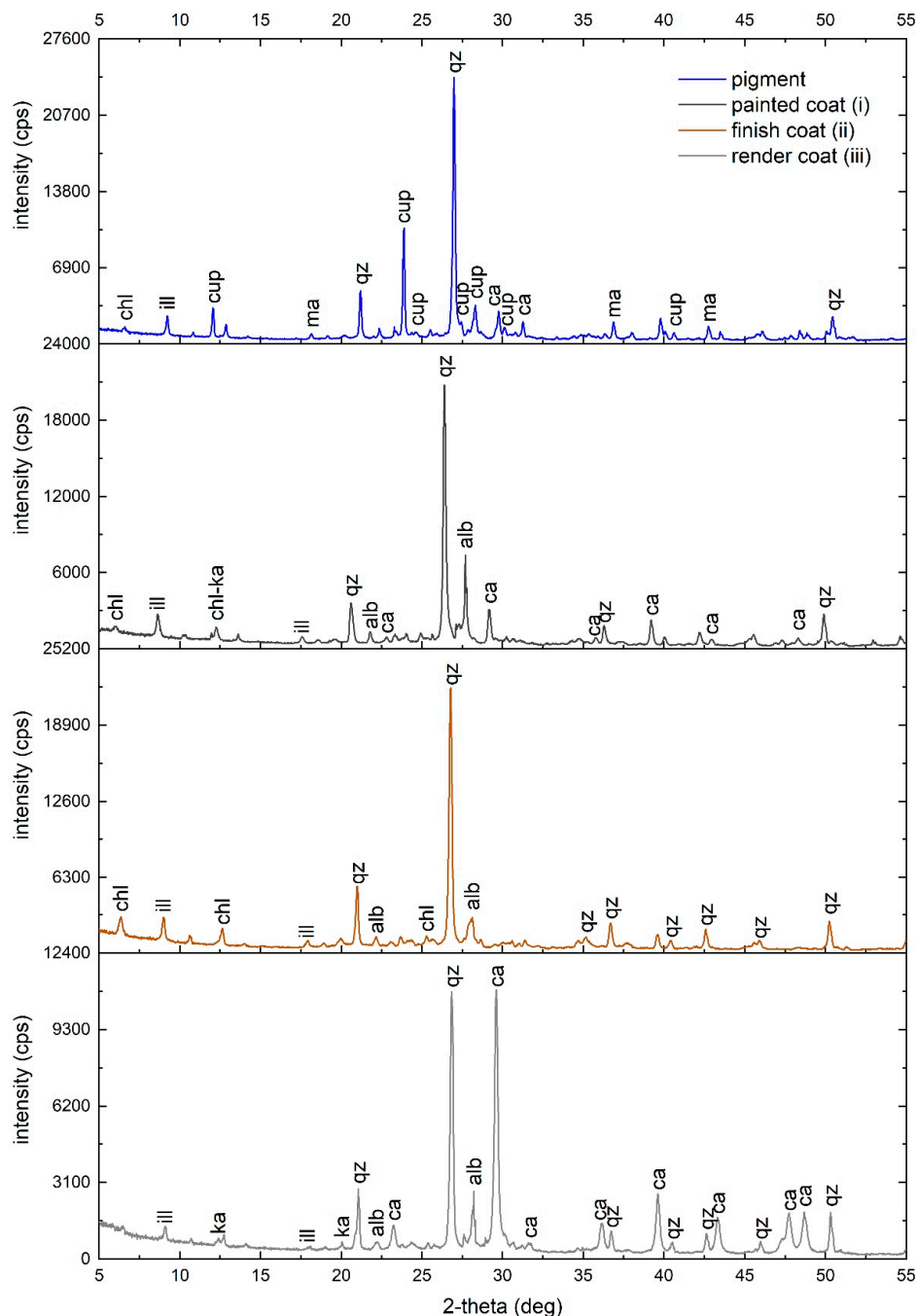


**Figure 6.** XRD analysis on powders of the different layers. From the top, the diffractograms of the pigment, the painted coat (i), the finish coat (ii) and the render coat (iii) can be seen, showing the main signals of the identified minerals. Legend: chl: chlorite; ill: illite; cup: cuprorivaite; ma: magnetite; qz: quartz; ca: calcite; ka: kaolinite; alb: albite.

We also used SEM-EDX on a polished cross section of the layer in order to obtain information on the pigments used. Particles containing copper, calcium and silicon were detected. Their qualitative and semiquantitative elemental composition is compatible with that of Egyptian blue. The blue pigment particles are not uniformly distributed over the entire surface and vary in size between 15 and 40  $\mu\text{m}$ . The absence of tin and zinc in

the EDX analyses proves the use of pure copper-based compounds as precursors for the synthesis of Egyptian blue [11].

Figure 7 shows a typical EDX spectrum of these particles, together with their elemental distribution map. Iron is widely present, likely due to the substrate or to the black pigment, which was identified as a black earth as also hypothesised by X-ray diffraction analysis. Figure 8 highlights some particles of Egyptian blue on the surface, as well as the general composition of the clay substrate, with silicon and aluminium being the most diffuse elements.

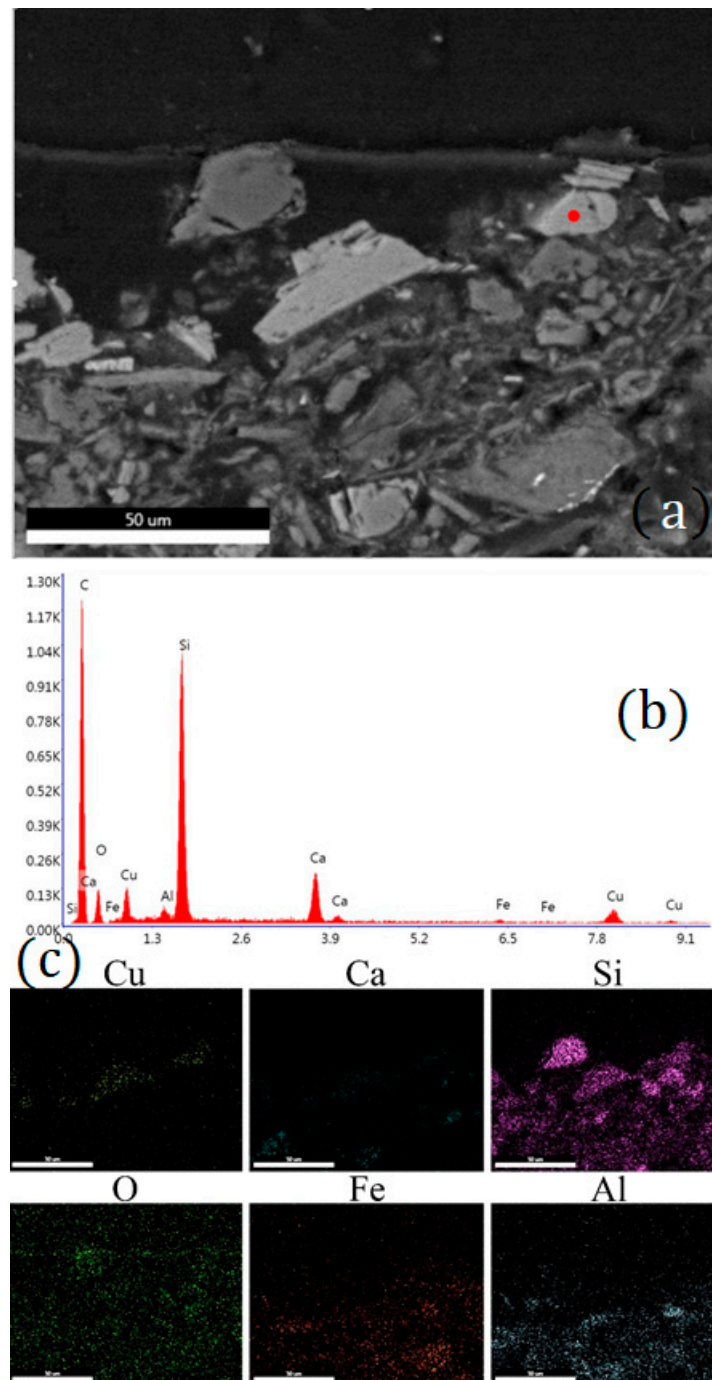


**Figure 7.** (a) SEM image in BSE mode of the painted layer; (b) EDX spectrum of a particle of Egyptian blue; (c) EDX elemental distribution maps (scale bar: 50 µm).

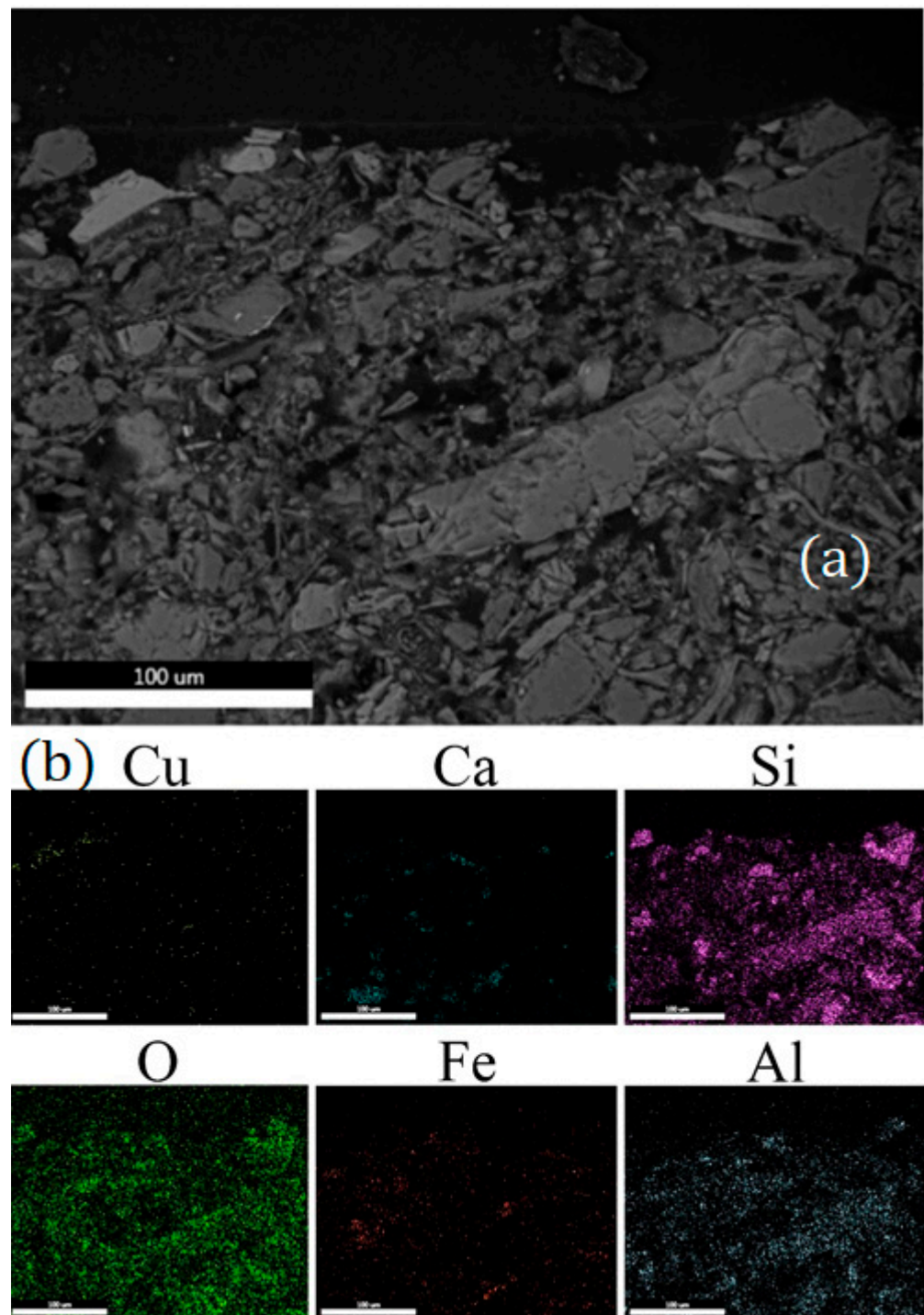


**Figure 8.** (a) SEM image in BSE mode of the painted layer and its substrate; (b) EDX elemental distribution maps (scale bar: 100 µm).

(ii) Finish coat

The thickness (11 mm) is almost homogeneous, the contact surface of the underlying coat is nearly flat, but it is marked by narrow cavities running parallel to the same surface.

The bulk is made of clay mud with many rounded (size 0.5–1 mm) and linear cavities (long and narrow—length about 10 mm) (Figure 3). The composition of the clay enlightened after the pre-treatment of the samples consists of: illite, chlorite and kaolinite together with angular quartz (size 0.05 mm) [23]. The XRD patterns are very similar to those shown in Figure 4. There are few signs of coarse clasts (gneiss with sub-angular corners, size 3.0 mm).

The texture is similar to the texture of the painted coat (i), and the different shape of cavities and the different percentage of coarse clasts are worth noting.

Some of the signals observed in the FTIR spectrum are those already observed in the painted coat, which are the peaks already attributed to calcium carbonate (1408, 872 and 712  $\text{cm}^{-1}$ ) and to quartz (797, 778 and 694  $\text{cm}^{-1}$ ), which make up the mortar. There are peaks at 3694, 3651, 3627 and 3618  $\text{cm}^{-1}$  (stretching of outer and inner hydroxyl ions), and 1084 and 1017  $\text{cm}^{-1}$  (Si–O stretching bands of quartz and kaolinite). These peaks are probably related to clay minerals, such as illite [26]. XRD analysis on powders revealed the presence of quartz, illite, albite and chlorite (Figure 6).

#### (iii) Render coat

The thickness (30 mm) shows some irregularities, but the contact surface with the underlying coat is quite flat.

The coat contains a Mg lime binder associated with an aggregate made of sub-rounded clasts of quartz, limestone, gneiss, serpentine etc. (sand from Pre-Alpine river deposits, low sorting, size 0.5–5.0 mm); the texture is marked by many rounded cavities of different shapes and sizes (0.2–1.2 mm) (Figure 3). This layer has commonly been detected in Roman plasters in Lombardy [5]. The FTIR analysis suggested the same composition as with the finish coat. XRD on powder analysis confirmed the presence of calcite, quartz, albite, kaolinite and illite (Figure 6).

## 4. Discussion

Vitruvius and Pliny recommended using clayey earth only for daubing on reeds, and the use in plaster as a render coat (i.e., southern *Gallia*) [14,33]. However, the plaster found at the site of *Santa Maria all Porta* shows the first detection in Roman Lombardy of a three-coat work (Figure 3), combining a finish coat and an intermediate coat, both containing clay with quartz and different proportions of coarse clasts (perhaps added to prevent cracking as the clay dries) and the proportion and shape of the cavities (possibly due to the presence of organic fibres?); these coats are lying on a render coat made, as usual, of lime and sandy aggregate.

Coats made of clay mud are extremely rare in the archaeological sites of Lombardy. A comparable case to date is a wall painting fragment (about 1.2–2 mm thick) pertaining to the wall plasters of the Republican Sanctuary of Brescia, built in the first half of the first century BCE. However, this differs greatly in the thickness of the painted layer and in the morphological features of the finish coat layer [14]. The painted coat of Brescia in fact supports a pigmented layer made of green earth and Egyptian blue and matches the features (composition, texture, presence of coarser clasts) of the painted coat found in Milan. A noticeable difference is the coat thickness (the coat from Milan is about two- or three-fold thick: 4 mm versus 1.2–2 mm). The finish coat shows a comparable texture as the previous one, however, with a considerably lower percentage of coarse clasts, and with the presence of elongated cavities. This is the first time that this kind of finish coat has been detected here in Roman Lombardy [14]. The render coat shows the same lithological composition and the same texture as already detected in equivalent coats of Roman Lombardy [5]. The features of the aggregate match those of the sands of the Pre-Alpine river deposits, diffused around Milan [5].

Regarding the provenance of the clay, the identification is uncertain as clay deposits are dispersed in the river Po alluvial plain in central and southern Lombardy: two areas near Milan, pertaining to this plain, were historically used to supply this raw material, mainly to make bricks. The first area is located in the north-western area of Milan and consists of a loessic-colluvial cover (2–3 m thick, clay) on glacio-fluvial deposits (weathered gravel) of middle Pleistocene. The second area is located near the southern border of the present-day metropolitan area and is made up of glacio-fluvial deposits of low energy (sand, silt and clayey silt) of upper Pleistocene [34].

With regard to the pigment determined in the fragments from Milan, Egyptian blue is the most common inorganic blue used by the Romans and is referred to as *caerulem*

*aegyptium* by both Pliny and Vitruvius [35,36]. The painting layer also contains magnetite (black earth), as highlighted by both the XRD and EDX results. The mixture of Egyptian blue with black, such as carbon or iron pigments, has already been identified in Roman painted surface samples [37] for example, at Paestum [38]. FTIR-ER analyses revealed organic compounds on the external surface, probably originally used as a surface treatment [14], and gypsum, likely due to decay phenomena [29].

## 5. Conclusions

The wall painting fragments excavated in the *Palatium* of *Mediolanum* show a stratigraphy combining a painted and a finish coat both containing clay mud and fine quartz, lying on a render coat made of lime and silicate sand. The pigment is a mixture of Egyptian blue and magnetite (black earth), which was a regular artistic practice as attested in the literature.

A similar painted coat was found in the wall plasters of the Republican Sanctuary of *Brixia*; however, a finish coat made of clay was detected here for the first time in terms of the plasters of Roman Lombardy. In particular, given the position of the coat in the plaster sequence from the site of *Santa Maria alla Porta*, it would seem to be an alternative to the coat called *marmoratum*, which was normally made of crushed calcite crystals and is almost always present in painted plasters throughout the Roman world.

Unfortunately, the plaster found in Milan was excavated from rubble: it is thus impossible to know the exact dating, the original location or the role of this particular kind of mortar in rendering the walls.

Finally, we believe this work provides an important contribution to the study of the entire sequence of creating plaster; a study frequently neglected in comparison with the emphasis on painted surfaces. The palette of pigments used in Roman wall paintings is widely documented, but the characteristics (texture and composition) of the mortar layers supporting the painting only derive from a few archaeological sites. The expansion of the knowledge of these characteristics to a great number of Roman sites, together with the relationships among different layers and different pigments, may help to understand the processes involved in painted plaster.

**Author Contributions:** Conceptualisation, R.B. and L.F.; investigation, R.B., L.F., C.C. and L.R.; writing—original draft preparation, R.B., L.F., C.C. and L.R.; writing—review and editing, R.B., L.F., C.C. and L.R. All authors have read and agreed to the published version of the manuscript.

**Funding:** This research received no specific grant from any funding agency in the public, commercial or not-for-profit sectors.

**Data Availability Statement:** The data presented in this study are available on request from the corresponding author.

**Acknowledgments:** The authors heartily acknowledge the Fondazione Banca del Monte di Lombardia and Norberto Masciocchi for support.

**Conflicts of Interest:** The authors declare no conflict of interest.

## References

1. Vitruvius. *On Architecture*; Schofield, R., Ed.; Penguin classics; Penguin Books Limited: London, UK, 2009; ISBN 9780141931951.
2. Pliny. *Natural History*; Eichholz, D.E., Ed.; Loeb Classical Library; Heinemann: Cambridge, UK, 1962.
3. Laurie, A.P. *Greek and Roman Methods of Painting: Some Comments on the Statements Made by Pliny and Vitruvius about Wall and Panel Painting*; Cambridge University Press: Cambridge, UK, 1910.
4. Bugini, R.; Folli, L.; Biondelli, D. Grain morphology of aggregates in Roman plasters. In Proceedings of the 14th Euroseminar on Microscopy on Applied to Building Materials, Helsingør, Denmark, 10–14 June 2013; Danish Technological Institute: Taastrup, Denmark, 2013; pp. 25–28.
5. Bugini, R.; Folli, L. Critères pour la comparaison des enduits peints romains de la Lombardie. *ArcheoSciences* **2013**, *37*, 41–50. [[CrossRef](#)]
6. Ergenç, D.; La Russa, M.F.; Ruffolo, S.A.; Fort, R.; Sánchez Montes, A.L. Characterization of the wall paintings in La Casa de los Grifos of Roman city Complutum. *Eur. Phys. J. Plus* **2018**, *133*, 355. [[CrossRef](#)]

7. Mateos, L.D.; Esquivel, D.; Cosano, D.; Jiménez-Sanchidrián, C.; Ruiz, J.R. Micro-Raman analysis of mortars and wall paintings in the Roman villa of Fuente Alamo (Puente Genil, Spain) and identification of the application technique. *Sens. Actuators A Phys.* **2018**, *281*, 15–23. [[CrossRef](#)]
8. Giorgi, L.; Nevin, A.; Nodari, L.; Comelli, D.; Alberti, R.; Gironde, M.; Mosca, S.; Zendri, E.; Piccolo, M.; Izzo, F.C. In-situ technical study of modern paintings part 1: The evolution of artistic materials and painting techniques in ten paintings from 1889 to 1940 by Alessandro Milesi (1856–1945). *Spectrochim. Acta Part A Mol. Biomol. Spectrosc.* **2019**, *219*, 530–538. [[CrossRef](#)]
9. Nodari, L.; Ricciardi, P. Non-invasive identification of paint binders in illuminated manuscripts by ER-FTIR spectroscopy: A systematic study of the influence of different pigments on the binders' characteristic spectral features. *Herit. Sci.* **2019**, *7*, 7. [[CrossRef](#)]
10. La Nasa, J.; Moretti, P.; Maniccia, E.; Pizzimenti, S.; Colombini, M.P.; Miliani, C.; Modugno, F.; Carnazza, P.; De Luca, D. Discovering Giuseppe Capogrossi: Study of the Painting Materials in Three Works of Art Stored at Galleria Nazionale (Rome). *Heritage* **2020**, *3*, 52. [[CrossRef](#)]
11. Pronti, L.; Romani, M.; Viviani, G.; Stani, C.; Gioia, P.; Cestelli-Guidi, M. Advanced methods for the analysis of Roman wall paintings: Elemental and molecular detection by means of synchrotron FT-IR and SEM micro-imaging spectroscopy. *Rend. Lincei Sci. Fis. Nat.* **2020**, *31*, 485–493. [[CrossRef](#)]
12. Sbroscia, M.; Cestelli-Guidi, M.; Colao, F.; Falzone, S.; Gioia, C.; Gioia, P.; Marconi, C.; Mirabile Gattia, D.; Loreti, E.M.; Marinelli, M.; et al. Multi-analytical non-destructive investigation of pictorial apparatuses of “Villa della Piscina” in Rome. *Microchem. J.* **2020**, *153*, 104450. [[CrossRef](#)]
13. Corcea, I.M.; Ghervase, L.; Țentea, O.; Pârău, A.C.; Rădvan, R. First Analytical Study on Second-Century Wall Paintings from Ulpia Traiana Sarmizegetusa: Insights on the Materials and Painting Technique. *Int. J. Archit. Herit.* **2020**, *14*, 751–761. [[CrossRef](#)]
14. Bugini, R.; Corti, C.; Folli, L.; Rampazzi, L. Unveiling the Use of Creta in Roman Plasters: Analysis of Clay Wall Paintings From Brixia (Italy). *Archaeometry* **2017**, *59*, 84–95. [[CrossRef](#)]
15. Germinario, C.; Francesco, I.; Mercurio, M.; Langella, A.; Sali, D.; Kakoulli, I.; De Bonis, A.; Grifa, C. Multi-analytical and non-invasive characterization of the polychromy of wall paintings at the Domus of Octavius Quartio in Pompeii. *Eur. Phys. J. Plus* **2018**, *133*, 359. [[CrossRef](#)]
16. Biron, C.; Mounier, A.; Arantegui, J.P.; Bourdon, G.L.; Servant, L.; Chapoulie, R.; Roldán, C.; Almazán, D.; Díez-de-Pinos, N.; Daniel, F. Colours of the «images of the floating world». Non-invasive analyses of Japanese ukiyo-e woodblock prints (18th and 19th centuries) and new contributions to the insight of oriental materials. *Microchem. J.* **2020**, *152*, 104374. [[CrossRef](#)]
17. Daveri, A.; Malagodi, M.; Vagnini, M. The Bone Black Pigment Identification by Noninvasive, In Situ Infrared Reflection Spectroscopy. *J. Anal. Methods Chem.* **2018**, *2018*, 6595643. [[CrossRef](#)]
18. Izzo, F.; Germinario, C.; Grifa, C.; Langella, A.; Mercurio, M. External reflectance FTIR dataset (4000–400  $\text{cm}^{-1}$ ) for the identification of relevant mineralogical phases forming Cultural Heritage materials. *Infrared Phys. Technol.* **2020**, *106*, 103266. [[CrossRef](#)]
19. Zuena, M.; Buemi, L.P.; Stringari, L.; Legnaioli, S.; Lorenzetti, G.; Palleschi, V.; Nodari, L.; Tomasin, P. An integrated diagnostic approach to Max Ernst's painting materials in his Attirement of the Bride. *J. Cult. Herit.* **2020**, *43*, 329–337. [[CrossRef](#)]
20. Rosi, F.; Miliani, C.; Delaney, J.; Dooley, K.; Stringari, L.; Subelyte, G.; Buemi, L.P. CHAPTER 1. Jackson Pollock's Drip Paintings: Tracing the Introduction of Alkyds Through Non-invasive Analysis of Mid-1940s Paintings. In *Science and Art; The Royal Society of Chemistry*: London, UK, 2020; pp. 1–18. ISBN 9781788016384.
21. Ranalli, G.; Zanardini, E.; Andreotti, A.; Colombini, M.P.; Corti, C.; Bosch-Roig, P.; De Nuntiis, P.; Lustrato, G.; Mandrioli, P.; Rampazzi, L.; et al. Hi-tech restoration by two-steps biocleaning process of Triumph of Death fresco at the Camposanto Monumental Cemetery (Pisa, Italy). *J. Appl. Microbiol.* **2018**, *125*, 800–812. [[CrossRef](#)]
22. Goldstein, J.I.; Newbury, D.E.; Michael, J.R.; Ritchie, N.W.M.; Scott, J.H.J.; Joy, D.C. *Scanning Electron Microscopy and X-ray Microanalysis*; Springer: New York, NY, USA, 2017; ISBN 9781493966769.
23. Thorez, J. *Phyllosilicates and Clay Minerals: A Laboratory Handbook for Their X-ray Diffraction Analysis*; Lelotte: Dison, Belgium, 1975.
24. Moore, D.M.; Reynolds, R.C., Jr. *X-ray Diffraction and the Identification and Analysis of Clay Minerals*; Oxford University Press: Oxford, UK, 1997; ISBN 9780195087130.
25. Farmer, V.C. *The Infrared Spectra of Minerals*; Mineralogical Society monograph; Mineralogical Society: London, UK, 1974; ISBN 9780903056052.
26. Wilson, M.J. *Clay Mineralogy: Spectroscopic and Chemical Determinative Methods*; Wilson, M.J., Ed.; Chapman & Hall: London, UK, 1994; ISBN 9780412533808.
27. Mirti, P.; Appolonia, L.; Casoli, A.; Ferrari, R.P.; Laurenti, E.; Amisano Canesi, A.; Chiari, G. Spectrochemical and structural studies on a roman sample of Egyptian blue. *Spectrochim. Acta Part A Mol. Biomol. Spectrosc.* **1995**, *51*, 437–446. [[CrossRef](#)]
28. Rampazzi, L.; Andreotti, A.; Bressan, M.; Colombini, M.P.; Corti, C.; Cuzman, O.; D'Alessandro, N.; Liberatore, L.; Palombi, L.; Raimondi, V.; et al. An interdisciplinary approach to a knowledge-based restoration: The dark alteration on Matera Cathedral (Italy). *Appl. Surf. Sci.* **2018**, *458*, 529–539. [[CrossRef](#)]
29. Ranalli, G.; Zanardini, E.; Rampazzi, L.; Corti, C.; Andreotti, A.; Colombini, M.P.; Bosch-Roig, P.; Lustrato, G.; Giantomassi, C.; Zari, D.; et al. Onsite advanced biocleaning system for historical wall paintings using new agar-gauze bacteria gel. *J. Appl. Microbiol.* **2019**, *126*, 1785–1796. [[CrossRef](#)]

30. Brunello, V.; Corti, C.; Sansonetti, A.; Tedeschi, C.; Rampazzi, L. Non-invasive FTIR study of mortar model samples: Comparison among innovative and traditional techniques. *Eur. Phys. J. Plus* **2019**, *134*, 270. [[CrossRef](#)]
31. Arrizabalaga, I.; Gomez-Laserna, O.; Carrero, J.A.; Bustamante, J.; Rodriguez, A.; Arana, G.; Madariaga, J.M.; Antonio Carrero, J.; Bustamante, J.; Rodriguez, A.; et al. Diffuse reflectance FTIR database for the interpretation of the spectra obtained with a handheld device on built heritage materials. *Anal. Methods* **2015**, *7*, 1061–1070. [[CrossRef](#)]
32. Bruni, S.; Cariati, F.; Casadio, F.; Toniolo, L. Spectrochemical characterization by micro-FTIR spectroscopy of blue pigments in different polychrome works of art. *Vib. Spectrosc.* **1999**, *20*, 15–25. [[CrossRef](#)]
33. Ramjoue, E. Quelques particularites techniques des fresques romaines de Vandoeuvres dans le Canton de Geneve. In *Roman Wall Painting*; Béarat, H., Ed.; Fribourg University, Institute of Mineralogy and Petrography: Fribourg, Switzerland, 1997; pp. 167–179.
34. Carta Geologica d'Italia (CARG) 1:50.000—Foglio Milano n. 118, Servizio Geologico d'Italia (Piacenza, Italia). Available online: <https://www.isprambiente.gov.it/Media/carg/lombardia.html> (accessed on 28 April 2021).
35. Gettens, R.J.; Stout, G.L. *Painting Materials: A Short Encyclopaedia*; Dover Publications: New York, NY, USA, 1966; ISBN 0486215970.
36. Riederer, J. Egyptian blue. In *Artists' Pigments. A Handbook of Their History and Characteristics—Vol. 3*; West FitzHugh, E., Ed.; National Gallery of Art, Washington and Oxford University Press: Oxford, UK, 1997; pp. 23–45. ISBN 9782970013204.
37. Edreira, M.C.; Feliu, M.J.; Fernández-Lorenzo, C.; Martín, J. Spectroscopic Study of Egyptian Blue Mixed with Other Pigments. *Helv. Chim. Acta* **2003**, *86*, 29–49. [[CrossRef](#)]
38. Alberghina, M.F.; Germinario, C.; Bartolozzi, G.; Bracci, S.; Grifa, C.; Izzo, F.; La Russa, M.F.; Magrini, D.; Massa, E.; Mercurio, M.; et al. Non-invasive characterization of the pigment's palette used on the painted tomb slabs at Paestum archaeological site. *IOP Conf. Ser. Mater. Sci. Eng.* **2020**, *949*, 012002. [[CrossRef](#)]